Li_2MoO_4 coated $LiNi_{0.5}Co_{0.2}Mn_{0.3}O_2$ microspheres with enhanced lithium storage performances

Dan Li[a], Hongrui Peng[b,*], Guicun Li[c,*]

College of Materials Science and Engineering, Qingdao University of Science and Technology, Qingdao 266042, PR China.

[a]e-mail: lidanx1992@163.com, [b]e-mail: penghongrui@qust.edu.cn,

[c]e-mail: guicunli@qust.edu.cn

Abstract. The pristine $LiNi_{0.5}Co_{0.2}Mn_{0.3}O_2$ microspheres (P-NCM523) have been synthesized by a solid state method. To improve the lithium storage performances, Li_2MoO_4 layer has been coated on the surface of P-NCM523 by the facile reaction between lithium residue and $H_3PO_4 \cdot _{12}MoO_3 \cdot _{24}H_2O$. The Li_2MoO_4 coating can not only remove the lithium residue, but also facilitate the lithium ion transport of P-NCM523 electrode. The Li_2MoO_4 coated $LiNi_{0.5}Co_{0.2}Mn_{0.3}O_2$ microspheres (C-NCM523) exhibits enhanced electrochemical energy performances compared to P-NCM523, including high capacity (175.2 mA h g^{-1} at 0.2 C), excellent rate capability (109 mA h g^{-1} at 8 C), and good cycling stability (97% discharge capacity retention after 50 cycles). The findings may open up new opportunities in designing high-performance layered oxide cathode materials for lithium ion batteries

Introduction

The demand for high energy and high power rechargeable lithium ion batteries is increasing urgently along with the fast development of electric vehicles (EVs), hybrid EVs (HEVs), and plug-I hybrid electric vehicles (PHEVs) [1][2].The main factor limiting the performance of lithium ion batteries is the cathode material, which directly determines the cycle performance, the specific energy density, cost, and safety of the battery [3-6]. Layered lithium-mixed transition metal oxides, $LiNi_xCo_yMn_{1-x-y}O_2$, have attracted significant interest due to their unique properties including high energy density, good cycling stability, low toxicity, and low cost [7-9]. In the series of cathode materials, Ni offers a high special capacity but poor thermal stability, Co provides increased electronic conductivity resulting in an excellent rate capability, while Mn maintains an excellent cycling performance and safety [10-13]. However, there remain challenges for $LiNi_xCo_yMn_{1-x-y}O_2$ materials. First, the intrinsic low Li^+ ion conductivity of $LiNi_xCo_yMn_{1-x-y}O_2$ causes the relatively poor electrochemical performance at high current density. Second, the instability of de-lithiated phase of $LiNi_xCo_yMn_{1-x-y}O_2$ in organic electrolyte caused by the high reactivity of Co^{4+} and Ni^{4+} leads to safety issues and capacity fading [14-18]. Third, the Li_2CO_3/LiOH layer and the NiO-like thin layer near the surfaces caused by the direct redox reaction between $LiNi_xCo_yMn_{1-x-y}O_2$ materials and the atmosphere are electrochemically inactive to lithium intercalation/de-intercalation, which is believed to be responsible for the capacity loss of the stored $LiNi_xCo_yMn_{1-x-y}O_2$ materials [19].

In face of the challenges for the $LiNi_xCo_yMn_{1-x-y}O_2$ materials, various methods such as surface modification, and ion doping have been demonstrated to be effective to improve electrochemical performances of $LiNi_xCo_yMn_{1-x-y}O_2$ materials. Surface modification that coated cathode materials with metal oxides, metal phosphates and metal fluorides, such as V_2O_5 [11], TiO_2 [16], CuO [20], Li_3PO_4 [21], $Li_3V_2(PO_4)_3$ [22], SiP_2O_7 [23], LaF_3 [24], MgF_2 [24], and AlF_3 [25], have been reported due to its simplicity and effectivity. Therefore, the effect of coating layer on cathodes is highly dependent on the specific coating material [24][26], coating content [27][28], and heat treatment conditions [21]. To synthesize high-quality $LiNi_xCo_yMn_{1-x-y}O_2$, excess lithium sources are usually necessary to compensate for the volatilization of lithium during the high-temperature

calcination process. The lithium residue is harmful to the electrochemical performances. However, the removal of lithium residue inspires us to design a new coating layer to improve the electrochemical performances of $LiNi_xCo_yMn_{1-x-y}O_2$. Herein, we report a facile route to the synthesis of C-NCM523 by the reaction between lithium residue and $H_3PO_{4.12}MoO_{3.24}H_2O$ (HPMO). The in-situ formed Li_2MoO_4 coating layer can serve as a good Li^+ ion conductor to improve the electrochemical performances of $LiNi_xCo_yMn_{1-x-y}O_2$. As expected, the C-NCM523 exhibit enhanced electrochemical energy performances including high capacity, excellent rate capability, and good cycling stability.

Experimental

Synthesis of P-NCM523

Spherical P-NCM523 was synthesized by solid state method, details of which are described as follow: Commercial available spherical $Ni_{0.5}Co_{0.2}Mn_{0.3}(OH)_2$ powder was mixed with Li_2CO_3 (5 wt % excess), and then preheated at 500 °C in air for 5 h, finally annealed at 830 °C for 15 h in air.

Synthesis of C-NCM523

In a typical synthesis of C-NCM523, 0.01 g HPMO was added into absolute ethanol with stirring for 10 min. After a yellow solution was obtained, 0.2 g P-NCM523 powders were dispersed in the solution. The suspension was gently stirred for 30 min and then heated to 70 °C. After the complete evaporation of the solvent, the remaining powder was calcined at 450 °C for 5 h for later use.

Materials characterization

The crystal structures of the obtained samples were characterized by powder X-ray diffraction (XRD, Rigaku D-max-γA XRD with Cu Kα radiation, λ=1.54178 Å). The morphologies and sizes of the obtained samples were measured by field-emission scanning electron microscopy (FE-SEM, JSM 6700F). Energy dispersive X-ray spectrometry (EDS, Oxford Instruments INCA) was employed to analyze the composition and element distribution of cathode materials.

Electrochemical test

The typical electrochemical properties of all the samples were measured in CR2032 coin cells. The working electrodes were prepared by mixing the samples, carbon black (Super-P), and poly vinyl difluoride (PVDF) at a weight ratio of 70:20:10 and pasting on to pure Al foil. Pure lithium foil was used as the counter electrode. The electrolyte consisted of a solution of 1 M $LiPF_6$ in ethylene carbonate (EC)/dimethyl carbonate (DMC) at a volume ratio of 1:1. The cells were assembled in an argon-filled glove box with the concentrations of moisture and oxygen below 1 ppm. The galvanostatic charge-discharge tests of the cells were carried out using LAND-CT2001A automatic battery tester at different current rates in the voltage range of 3.0–4.3 V. The cyclic voltammetry (CV) curves were recorded by using PGSTAT302 N electrochemical workstation in the voltage range of 3.0–4.3 V at the scanning rate of 0.5 mV s^{-1}. The electrochemical impedance spectroscopy (EIS) was performed in the frequency range from 10^{-3} Hz to 105 Hz at open circuit voltage by applying a 5 mV signal.

Results and discussion

Structure and morphology of materials

Fig. 1A shows the powder XRD patterns of the P-NCM523 and C-NCM523. It is found that all the observed diffraction peaks of the P-NCM523 can be indexed to a hexagonal α-NaFeO$_2$ structure with space group R-3m [29]. The well-defined XRD pattern displays the hexagonal doubles (006)/(102) and (108)/(110) with clear splits, indicating that the P-NCM523 has good hexagonal ordering and good layered characteristics. The ratio of $I(003)/I(104)$ is 1.36, indicating the desirable cation mixing of the $LiNi_{0.5}Co_{0.2}Mn_{0.3}O_2$ sample [31]. The diffraction peaks appear to be almost identical for all the C-NCM523, revealing that there is no change in the crystalline structure of P-NCM523 after coating. For 5 wt % Li_2MoO_4 coated P-NCM523, only a small peak appears at about 21.03°. To determine the coating layers, XRD pattern of the 10 wt % Li_2MoO_4 coated P-NCM523 shows that the small peaks in the range of 20−36° are the reflection of rhombohedral

Li_2MoO_4 phase (JCPDS No 12-0763). It should be noted that no other diffraction peaks corresponding to phosphate were found, presumably due to the low loading content of HPMO. The results demonstrate that Li_2MoO_4 coating layer has been formed by the reaction between lithium residue and HPMO. The rhombohedral Li_2MoO_4 has been reported as the anode material for lithium ion battery, which is favorable for the transport of the Li^+ ions [30].
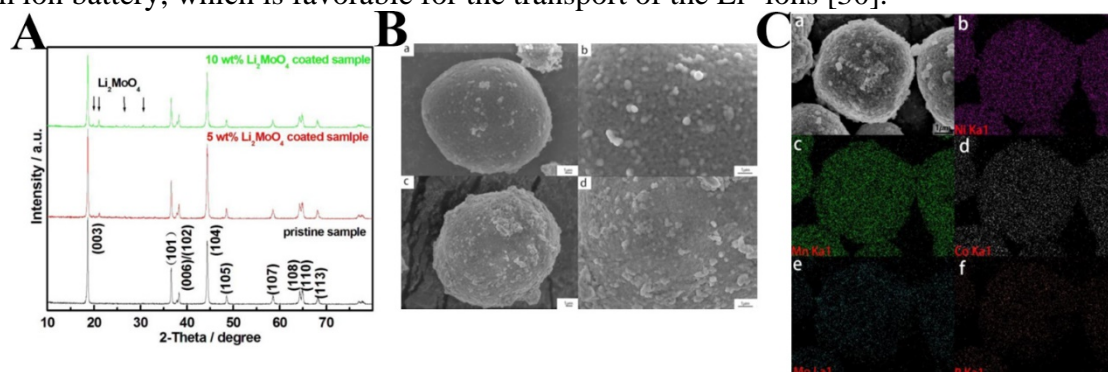
Fig. 1 XRD patterns (A) and SEM images (B) of the P-NCM523 and C-NCM523, EDS element mapping (C) of C-NCM523.

It can be seen in Fig. 1B that the P-NCM523 and C-NCM523 exhibit spherical morphologies with diameters of about 20 μm. The spherical morphologies of the P-NCM523 is derived from the spherical $Ni_{0.5}Co_{0.2}Mn_{0.3}(OH)_2$ precursor. High-magnification SEM images in Fig. 1B (b) and d reveal that the P-NCM523 and C-NCM523 are composed of numerous primary nanoparticles. It is clear that the surface of C-NCM523 is much rougher than that of the P-NCM523 due to the presence of Li_2MoO_4 coating layer. In order to further confirm the uniform coating of Li_2MoO_4 on the surface of P-NCM523, EDS mapping was carried out. SEM image with EDS mapping for C-NCM523 is shown in Fig. 1C. The EDS mapping images reveal that Mo and P mapping have the same shape a the cathode material particle, indicating that there is a homogeneous distributed Li_2MoO_4 coating layer through the P-NCM523, which can serve as a protection material to improve the electrochemical performances

Electrochemical performance

To investigate the effect of the Li_2MoO_4 coating layer on the electrochemical properties of $LiNi_{0.5}Co_{0.2}Mn_{0.3}O_2$ microspheres, the CV, galvanostatic discharge-charge, and EIS tests were performed and evaluated in lithium half-cells. Fig. 2a and 2b compares the CV profiles of the pristine and C-NCM523 electrodes in the first four scans cycled in the voltage range of 3.0–4.3 V (vs. Li/Li^+). For the C-NCM523, a couple of oxidation and reduction peaks appear at 3.878 V and 3.700 V in the first cycle, which correspond to the redox reaction of Ni^{2+}/Ni^{4+}, because the Jahn-Teller distortion of Ni^{3+} (d7) in NiO_6 octahedra leads to the direct oxidation of Ni^{2+} to Ni^{4+} [18]. The oxidation peak are shifted to 3.837 V in the second cycle and 3.817 V in the third cycle after the initial activation and stabilization of the active materials. For the P-NCM523, the oxidation peaks are located at 3.874, 3.837, 3.805 and 3.805 V for the first four scan cycles, respectively, while the reduction peaks appear at 3.671 V. For all samples, no considerable change in the position or the intensity of the peak in the fourth cycle is observed, indicating that the initial layered crystal structures of the C-NCM523 and the P-NCM523 are maintained without phase transition. However, it is obvious that the gap between the redox peaks for the C-NCM523 electrode (0.117 V) is smaller than that of the P-NCM523 electrode (0.134 V), demonstrating the coated electrode shows better electrode kinetics due to a lower degree of polarization of the electrode. On the other hand, the reduction peak shape and intensity of the C-NCM523 electrode in the first four scans have little change compared with the pristine electrode, indicating that the reversibility of the former electrode is much better than that of the P-NCM523.
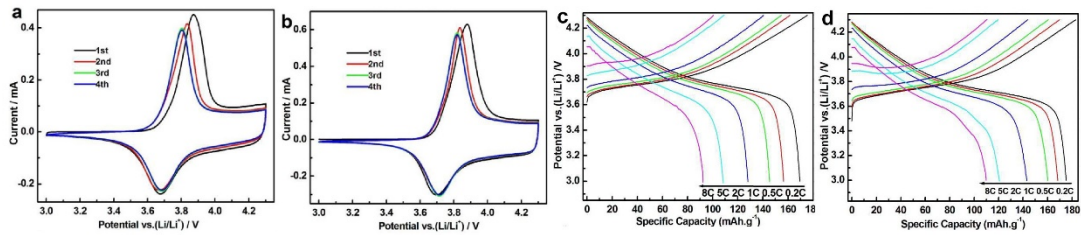
Fig. 2 CV curves (between 3 and 4.3 V at a scan rate of 0.1 mV s^{-1}) and Galvanostatic charge-discharge curves of the P-NCM523 (a, c) and C-NCM523 (b, d)

The charge-discharge curves of the pristine and the C-NCM523 electrodes in the voltage range of 3.0–4.3 V at different current rates are presented in Fig. 2c and 2d. It is obvious that the discharge capacities both the P-NCM523 and C-NCM523 electrodes are all decreased as the current rates increased. At 0.2 C (1 C = 160 mA g^{-1}), the C-NCM523 electrode delivers an initial discharge capacity of 176.9 mA h g^{-1}, which is higher than that of the P-NCM523 electrode (169.7 mA h g^{-1}). At 0.5, 1, 2, 5, and 8 C, the corresponding discharge capacities for the C-NCM523 electrode are 168.4, 160.2, 143.1, 120.7, and 109.9 mA h g^{-1}, respectively, which is higher than the P-NCM523 electrodes (156.4, 145.4, 128.1, 108.5 and 91.7 mA h g^{-1}, respectively).

The distinct decrease in discharge capacity of P-NCM523 is due to the slow kinetics at high rates and the destruction of the surface resulting from the side reactions between the cathode and electrolyte [32]. Fig. 3a shows the rate capacity of the pristine and the C-NCM523 electrodes at different current rates from 0.2 to 8 C. It is clear that the discharge capacities of the C-NCM523 electrode are higher than that of the P-NCM523electrode at various current rates, revealing its superior rate capability. When the current rate reverses back to 0.2 C, the discharge capacity of the C-NCM523 electrode can recover to 175.5 mA h g^{-1} and the corresponding capacity retention rate is 99.2% with respect to the initial cycle at 0.2 C. However, the discharge capacity and the corresponding capacity retention rate of the P-NCM523electrode are 167.3 mA h g^{-1} and 98.5%, respectively. It is indicated that the C-NCM523 electrode materials possess high structure stability even after high rate cycling. Fig. 3b gives the long-term cycling performances of the pristine and the C-NCM523 electrodes in the voltage range of 3.0–4.3 V at the 1 C current rate. In the case of the C-NCM523 electrode, the initial capacity is 161.3 mA h g^{-1} (1 C current rate), which decreases to 156.6 mA h g^{-1}, with a good capacity retention of 97.0% after 50 cycles. However, for the pristine sample, the initial capacity is 146.7 mA h g^{-1} (1 C current rate), which decreases to 137.7 mA h g^{-1} after 50 cycles, with an inferior capacity retention of 93.8%. Those results demonstrate that Li$_2$MoO$_4$ coating layer can prevent the side reactions between the cathode and electrolyte and facilitate the lithium ion diffusion kinetics especially at high rates. And all of those were clearly observed that the C-NCM523 electrode has better electrochemical performances including the rate capability and the cycle stability than the pristine electrode, especially at high current rates.
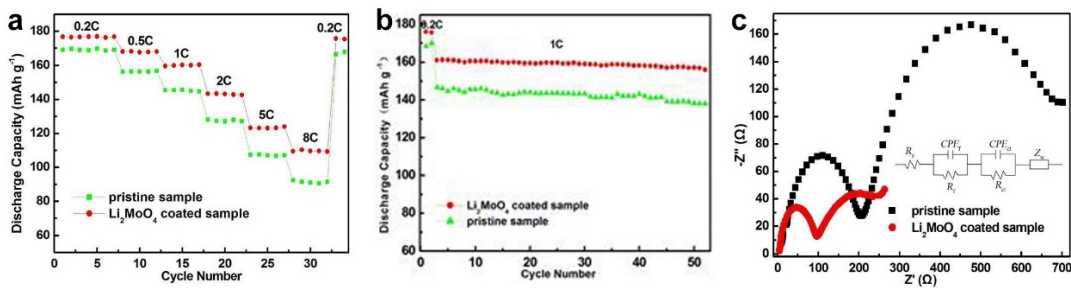
Fig. 3 Cycle performance (a) at different current rates and long-term cycling performances (b) at 1 C of the pristine and C-NCM523 electrodes in the voltage range of 3.0–4.3 V, (c) Nyquist plots of the pristine and C-NCM523 electrodes and equivalent circuit model.

Fig. 3c shows the EIS curves of the pristine and the C-NCM523 electrodes in the discharged state of 3.0 V after 50 cycles. The inset in Fig. 3c shows the equivalent circuits of the C-NCM523 and the C-NCM523 electrodes (CPE is the corresponding constant phase element and the Warburg impedance (Zw) is related to the solid-state diffusion of lithium ions into the material). Each of the curves with a frequency range from 10^5 to 10^{-3} Hz consists of two semicircles. The first semicircle

in the high frequency is related with the resistance for Li^+ ion migration through the surface film (Rf) and film capacitance, while the second one in the low frequency with charge transfer resistance (Rct) [33][34]. The C-NCM523 electrode exhibits much lower Rf (80.1 Ω) and Rct (257 Ω) in comparison with the pristine electrode (211 Ω for Rf and 530 Ω for Rct), which suggests that the Li_2MoO_4 coating layer can facilitate the lithium ion transport of P-NCM523 electrode. On the other hand, the Li_2MoO_4 coating layer can protect the P-NCM523 electrode from side reactions on the surface of the P-NCM523 and hence prevents the metal ions from being dissolved into the liquid electrolyte. The results encourage us to believe that the Li_2MoO_4 layer on $LiNi_{0.5}Co_{0.2}Mn_{0.3}O_2$ does not block a Li^+ intercalation, but rather function as an expediter for Li^+ transport to the host structures.

Conclusion

In conclusion, we have developed a Li_2MoO_4 surface modification route to improve the electrochemical performance of $LiNi_{0.5}Co_{0.2}Mn_{0.3}O_2$ microspheres. The Li_2MoO_4 coating layer formed by the reaction between lithium residue and $H_3PO_{4.12}MoO_{3.24}H_2O$ can facilitate the lithium ion transport of $LiNi_{0.5}Co_{0.2}Mn_{0.3}O_2$ electrode. As expected, the C-NCM523 exhibit enhanced lithium storage performances in comparison with the P-NCM523. The enhanced rate capability and cycle stability of the C-NCM523 can be attributed to the Li_2MoO_4 surface modification, which both suppressed the side reaction and facilitate ionic diffusion of Li^+ in the interface between the cathode and electrolyte. The findings can open up new opportunities in designing high-performance layered oxide cathode materials for lithium ion batteries.

Acknowledgement

References

[1] Zeheng Yang , et al. Stepwise co-precipitation to synthesize $LiNi_{1/3}Co_{1/3}Mn_{1/3}O_2$ one-dimensional hierarchical structure for lithium ion batteries [J]. J. Power Sources, 2014:272: 144-151.

[2] Haijun Yu, et al. Study of the lithium/nickel ions exchange in the layered $LiNi_{0.42}Mn_{0.42}Co_{0.16}O_2$ cathode material for lithium ion batteries: experimental and first-principles calculations [J]. Energy Environ. Sci. 2014 (3)1068 -1078.

[3] Xiukang Yang, et al. Spherical lithium-rich layered $Li_{1.13}[Mn_{0.534}Ni_{0.233}Co_{0.233}]_{0.87}O_2$ with concentration-gradient outer layer as high-performance cathodes for lithium ion batteries [J]. J. Power Sources, 2013:232:338-347.

[4] Xiukang Yang, et al. Layered $Li[Ni_{0.5}Co_{0.2}Mn_{0.3}]O_2$-$Li_2MnO_3$ core–shell structured cathode material with excellent stability [J]. J. Power Sources, 2013:242: 589-596.

[5] Sung-Kyun Jung, et al. Understanding the Degradation Mechanisms of $LiNi_{0.5}Co_{0.2}Mn_{0.3}O_2$ Cathode Material in Lithium Ion Batteries [J]. Adv. Energy Mater. 2014:4 (1):94-98.

[6] Tae-Hyung Cho, et al. Preparation and characterization of layered $LiMn_{1/3}Ni_{1/3}Co_{1/3}O_2$ as a cathode material by an oxalate co-precipitation method [J]. J. Power Sources 2006:159 (2):1322-1327.

[7] Zhongzhen Wu, et al. Depolarized and Fully Active Cathode Based on $Li(Ni_{0.5}Co_{0.2}Mn_{0.3})O_{-2}$ Embedded in Carbon Nanotube Network for Advanced Batteries [J].Nano Lett. 2014:14 (8):4700-4706.

[8] Peiyu HouDesign, et al. synthesis, and performances of double-shelled $LiNi_{0.5}Co_{0.2}Mn_{0.3}O_2$ as cathode for long-life and safe Li-ion battery [J]. J. Power Sources, 2014:265:174-181.

[9] Mijung Noh, Jaephil Cho, Optimized Synthetic Conditions of $LiNi_{0.5}Co_{0.2}Mn_{0.3}O_2$ Cathode Materials for High Rate Lithium Batteries via Co-Precipitation Method [J]. J. Electrochem. Soc. 2012:160 (1):A105-A111.

[10] Longwei Liang, et al. Co–precipitation synthesis of $Ni_{0.6}Co_{0.2}Mn_{0.2}(OH)_2$ precursor and characterization of $LiNi_{0.6}Co_{0.2}Mn_{0.2}O_2$ cathode material for secondary lithium batteries [J]. Electrochim. Acta, 2013:130:82-89.

[11] Xunhui Xiong, et al. Enhanced electrochemical properties of lithium-reactive V_2O_5 coated on the $LiNi_{0.8}Co_{0.1}Mn_{0.1}O_2$ cathode material for lithium ion batteries at 60 °C [J]. J. Mater. Chem. A, 2013 (4) 1284-1288.

[12] Zongyi Wang, et al. Infiltrative coating of $LiNi_{0.5}Co_{0.2}Mn_{0.3}O_2$ microspheres with layer-structured $LiTiO_2$: towards superior cycling performances for Li-ion batteries [J]. J. Mater. Chem. A, 2014 (47) 19983-19987.

[13] Fang Fu, et al. A hierarchical micro/nanostructured $0.5Li_2MnO_3 \cdot 0.5LiMn_{0.4}Ni_{0.3}Co_{0.3}O_2$ material synthesized by solvothermal route as high rate cathode of lithium ion battery [J]. Electrochem. Commun. 2014:44:54-58.

[14] Jun, Lu, et al. Nanoscale coating of $LiMO_2$ (M = Ni, Co, Mn) nanobelts with Li^+-conductive Li_2TiO_3: toward better rate capabilities for Li-ion batteries [J]. J. Am. Chem. Soc. 2013:135 (6) 1649-1652.

[15] Ke Du, et al. A high-powered concentration-gradient $Li(Ni_{0.85}Co_{0.12}Mn_{0.03})O_2$ cathode material for lithium ion batteries [J]. J. Power Sources, 2014:263:203-208.

[16] Yanping Chen, et al. An approach to application for $LiNi_{0.6}Co_{0.2}Mn_{0.2}O_2$ cathode material at high cutoff voltage by TiO_2 coating [J]. J. Power Sources, 2014:263:20-27.

[17] Hyung-Joo Noh, et al. High-Energy Layered Oxide Cathodes with Thin Shells for Improved Surface Stability [J]. Chem. Mater. 2014:26 (20):5973-5979.

[18] Yang-Kook Sun, et al. Cobalt-Free Nickel Rich Layered Oxide Cathodes for Lithium-Ion Batteries [J].ACS applied materials & interfaces, 2013:5(21):11434-11440.

[19] Ting Liu, et al. CuO-coated $Li[Ni_{0.5}Co_{0.2}Mn_{0.3}]O_2$ cathode material with improved cycling performance at high rates [J]. Electrochim. Acta，2012：85：605-611.

[20] Mi-Hee Park, et al. Flexible High-Energy Li-Ion Batteries with Fast-Charging Capability [J]. Nano Lett. 2014:14 (7):4083-4089.

[21] Han Gab Song, et al. Enhanced electrochemical properties of $Li(Ni_{0.4}Co_{0.3}Mn_{0.3})O_2$ cathode by surface modification using Li_3PO_4-based materials [J]. J. Power Sources, 2011:196 (16):6847-6855.

[22] Yi Liu, Xiao Huang, et al. $Li_3V_2(PO_4)_3$-coated $Li_{1.17}Ni_{0.2}Co_{0.05}Mn_{0.58}O_2$ as the cathode materials with high rate capability for Lithium ion batteries [J]. Electrochim. Acta.2014:147:696-703.

[23] Yong-Seok Lee, Docheon Ahn, et al. Improved Rate Capability and Thermal Stability of $LiNi_{0.5}Co_{0.2}Mn_{0.3}O_2$ Cathode Materials via Nanoscale SiP_2O_7 Coating [J]. J. Electrochem. Soc. 2011:158: A1354-A1360.

[24] Han Gab Song, Seuk Boum Kim, et al. Enhanced electrochemical properties of $Li[Ni_{0.5}Co_{0.2}Mn_{0.3}]O_2$ cathode by surface coating using LaF_3 and MgF_2 [J]. J. Electroceram.2012:29 (2):163-169.

[25] Yang-Kook Sun, Min-Joon Lee, et al. The Role of AlF_3 Coatings in Improving Electrochemical Cycling of Li-Enriched Nickel-Manganese Oxide Electrodes for Li-Ion Batteries [J]. Adv. Mater. 2012:24 (9):1192-1196.

[26] K. Karthikeyan, S. Amaresh, et al. Li(Mn$_{1/3}$Ni$_{1/3}$Fe$_{1/3}$)O$_2$–Polyaniline hybrids as cathode active material with ultra-fast charge–discharge capability for lithium batteries [J]. J. Power Sources. 2013:232: 240-245.

[27] Ting Shi, Yue Dong, et al. Enhanced cycle stability at high rate and excellent high rate capability of La$_{0.7}$S$_{r0.3}$Mn$_{0.7}$Co$_{0.3}$O$_3$-coated LiMn$_2$O$_4$ [J]. J. Power Sources. 2015:273:959-965.

[28] Qiang Fu, Fei Du, Xiaofei Bian, et al. Electrochemical performance and thermal stability of Li$_{1.18}$Co$_{0.15}$Ni$_{0.15}$Mn$_{0.52}$O$_2$ surface coated with the ionic conductor Li$_3$VO$_4$ [J]. J. Mater. Chem. A.2014:2:7555-7562.

[29] Xiukang Yang, Ruizhi Yu, et al. Facile synthesis and performances of nanosized Li$_2$TiO$_3$-based shell encapsulated LiMn$_{1/3}$Ni$_{1/3}$1Co$_{1/3}$O$_2$ microspheres [J]. J. Mater. Chem. A. 2014:2:8362-8368.

[30] Xudong Liu, Yingchun Lyu, et al. Nanotube Li$_2$MoO$_4$: a novel and high-capacity material as a lithium-ion battery anode [J]. Nanoscale.2014:6:13660-13667.

[31] K.K.Cheralathan, Na Young Kang, et al. Preparation of spherical LiNi$_{0.80}$Co$_{0.15}$Mn$_{0.05}$O$_2$ lithium-ion cathode material by continuous co-precipitation [J]. J. Power Sources.2010:195 (5): 1486-1494.

[32] Yuanlu Yao, Huaicheng Liu, et al. Synthesis and electrochemical performance of phosphate-coated porous LiNi$_{1/3}$Co$_{1/3}$Mn$_{1/3}$O$_2$ cathode material for lithium ion batteries [J]. Electrochim. Acta 2013:113:340-345.

[33] Huang J, Luo J. A facile and generic method to improve cathode materials for lithium-ion batteries via utilizing nanoscale surface amorphous films of self-regulating thickness [J]. Phys. Chem. Chem. Phys.2014:16 (17):7786-7798.

[34] Hyung-Joo Noh, Jin Wook Ju, et al. Comparison of Nanorod-Structured Li[Ni$_{0.54}$Co$_{0.16}$Mn$_{0.30}$]O$_2$ with Conventional Cathode Materials for Li-Ion Batteries [J]. ChemSusChem. 2014:7 (1):245-252.